



Contents lists available at ScienceDirect

Bioorganic & Medicinal Chemistry

journal homepage: www.elsevier.com/locate/bmc

FRET-based sensors for the human M₁-, M₃-, and M₅-acetylcholine receptors

Nicole Ziegler[†], Julia Bätz[†], Ulrike Zabel, Martin J. Lohse, Carsten Hoffmann^{*}

Department of Pharmacology and Toxicology, University of Wuerzburg, Versbacher Str. 9, 97078 Wuerzburg, Germany

ARTICLE INFO

Article history:

Received 28 April 2010

Revised 15 July 2010

Accepted 26 July 2010

Available online 30 July 2010

Keywords:

GPCR

Receptor activation

Muscarinic acetylcholine receptor

FRET

FIAsh-EDT₂

ABSTRACT

Based on the recently developed approach to generate fluorescence resonance energy transfer (FRET)-based sensors to measure GPCR activation, we generated sensor constructs for the human M₁-, M₃-, and M₅-acetylcholine receptor. The receptors were labeled with cyan fluorescent protein (CFP) at their C-terminus, and with fluorescein arsenical hairpin binder (FIAsh) via tetra-cysteine tags inserted in the third intracellular loop. We then measured FRET between the donor CFP and the acceptor FIAsh in living cells and real time. Agonists like acetylcholine, carbachol, or muscarine activate each receptor construct with half-maximal activation times between 60 and 70 ms. Removal of the agonist caused the reversal of the signal. Compared with all other agonists, oxotremorine M differed in two major aspects: it caused significantly slower signals at M₁- and M₅-acetylcholine receptors and the amplitude of these signals was larger at the M₁-acetylcholine receptor. Concentration–response curves for the agonists reveal that all agonists tested, with the mentioned exception of oxotremorine M, caused similar maximal FRET-changes as acetylcholine for the M₁-, M₃- and M₅-acetylcholine receptor constructs. Taken together our data support the notion that orthosteric agonists behave similar at different muscarinic receptor subtypes but that kinetic differences can be observed for receptor activation.

© 2010 Elsevier Ltd. All rights reserved.

1. Introduction

The G protein-coupled receptor (GPCR) superfamily is a major target for current drug treatment¹ and the family of muscarinic acetylcholine receptors (mACh) holds great promise for novel treatments of diseases like Alzheimer's disease, schizophrenia, obstructive pulmonary disease, diabetes as well as drug addiction and withdrawal.² Muscarinic ACh receptors are activated by the endogenous ligand acetylcholine and can be divided into two groups. The first group consists of the M₁-, M₃-, and M₅-ACh receptors that couple mainly to G_q-proteins, whereas the second group consists of the M₂-, and M₄-ACh receptors which mainly couple to G_i-proteins.³ However, given the high sequence similarity of mACh receptors it has proven difficult to develop sub-type selective ligands for these receptors.⁴ During the search for selective ligands it was discovered that modulators of these receptors can bind to allosteric binding sites in extracellular receptor parts⁵ with less sequence conservation and this lead to the development of allosteric modulators with some receptor sub-type selectivity.^{6–10} Most of

these analyses were done using assays like receptor radioligand binding or kinetic binding and/or dissociation experiments.¹¹

We have recently developed an approach for the study of receptor activation and signaling that is based on fluorescence resonance energy transfer (FRET) between two fluorophores and allows to monitor conformational changes in GPCRs in living cells.^{12–14} FRET is the radiation free energy transfer from an excited donor to an acceptor molecule via long range dipole–dipole coupling mechanisms. The initially developed approach for GPCRs utilized the fluorescent proteins CFP and YFP.¹² However, the insertion of the relatively large fluorescent proteins into an intracellular receptor loop may reduce their ability to couple to G-proteins. Thus, the approach was further developed by replacing the large YFP protein with the spectrally similar small fluorescein arsenical hairpin binder (FIAsh).¹⁵ This exchange improved the receptor coupling to G-proteins and CFP/FIAsh constructs often revealed larger agonist induced FRET-changes.^{13,14,16,17} FIAsh can be used to covalently label a specific motif (CCPGCC) which can be inserted into the 3rd intracellular loop (IL) of receptors.¹³ We have successfully applied this approach to the adenosine A_{2A} receptor,¹³ the α_{2A}-adrenergic receptor,^{13,14,16} and the M₂-ACh receptor.¹⁷

Here, we report the development of CFP/FIAsh-based receptor sensors for the human M₁-, M₃-, and M₅-ACh receptors. These sensors were used to monitor concentration-dependent effects of receptor modulation by orthosteric ligands in real time. Analysis of receptor kinetics induced by orthosteric ligands in living cells supports the view that receptor modulation results in a very rapid

Abbreviations: Carb, carbachol; CFP, cyan fluorescent protein; DMEM, Dulbecco's modified Eagle's medium; FCS, fetal calf serum; FIAsh, fluorescein arsenical hairpin binder; FRET, fluorescence resonance energy transfer; GPCR, G protein-coupled receptor; HBSS, Hank's balanced salt solution; mACh, muscarinic acetylcholine receptor; OxoM, oxotremorine M.

^{*} Corresponding author. Tel.: +49 931 201 48304; fax: +49 931 201 48539.

E-mail address: C.Hoffmann@toxi.uni-wuerzburg.de (C. Hoffmann).

[†] These authors contributed equally.

manner, and also revealed differences of orthosteric ligands at the different receptor subtypes.

2. Results

2.1. Design of the FRET-based muscarinic ACh receptor sensors

We created receptor constructs in which the whole amino acid sequence of the M₁-, M₃-, or M₅-ACh receptor was directly fused to the N-terminus of CFP using the additional amino acid sequence Ser/Arg encoding for an XbaI site. Unlike for the recently published M₂-ACh receptor FRET-sensor,¹⁷ expression of these constructs

was at the cells surface and no further export signal at the N-terminus was needed. To improve FRET efficiency we truncated the third intracellular loop (IL3) as described in detail for each construct in Section 5.1 and inserted instead the short tetra-cysteine motif CCPGCC for specific binding of FIAsh.¹⁵ It has previously been described that the third loop of mACh receptors can be deleted without loss of function,^{18,19} and we made sure that the described interaction sites for G-protein coupling were left intact.¹⁸ A schematic representation of the constructs is shown in Figure 1A. Next, all three receptor constructs were transfected in HEK-293 cells and expression at the plasma membrane was verified by means of confocal microscopy (Fig. 1B). As previously shown for several other

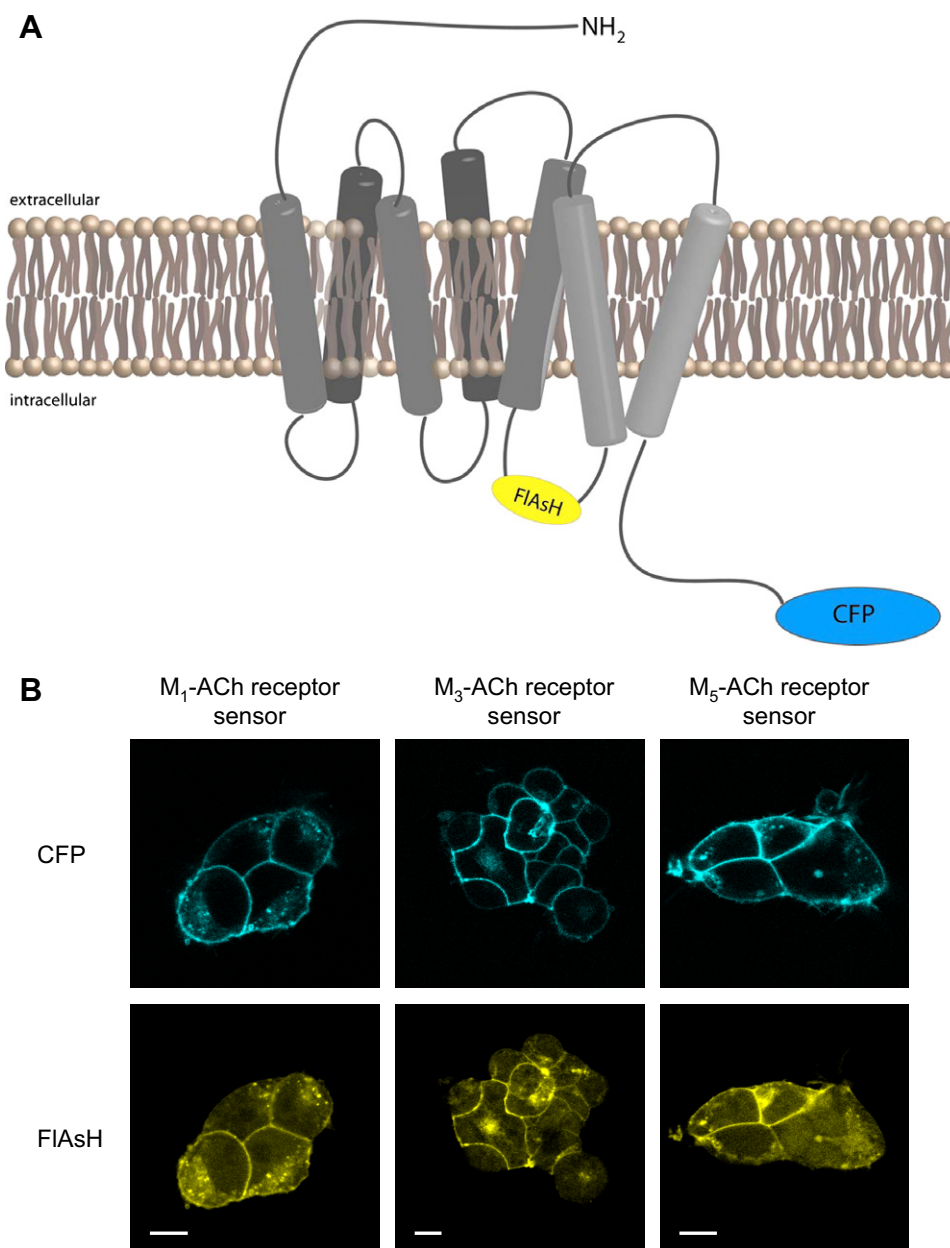


Figure 1. Generation and expression of the muscarinic M₁-, M₃-, and M₅-ACh receptor sensors. (A) General schematic structure of the receptor sensors. The cyan fluorescent protein was fused to the C-terminus of the respective human muscarinic ACh receptor subtype via a Ser/Arg amino acid sequence coding for an XbaI restriction site. In the M₁-ACh receptor the FIAsh binding motif CCPGCC was introduced into the shortened IL 3 between amino acid position G²²⁸ and K³⁵⁰, thus the novel sequence reads LAALQC²²⁸CCPGCCSGK³⁵⁰PRGKE. In the M₃-ACh receptor the FIAsh binding motif CCPGCC was introduced into the shortened IL 3 between amino acid position A²⁷¹ and A⁴⁶⁵, thus the novel sequence reads LAGLQA²⁷¹CCPGCCF⁴⁶⁵ALKTRS. In the M₅-ACh receptor the FIAsh binding motif CCPGCC was introduced into the shortened IL 3 between amino acid position G²³³ and N⁴²², thus the novel sequence reads KDLADLQ²³³GCCPGCCSGN⁴²²PNPSH as described in detail in Section 5. (B) HEK-293 cells were transfected with the corresponding sensor construct and analyzed by laser scanning microscopy. Confocal pictures show a distinct membrane expression of each respective receptor sensor as indicated by localization of CFP and selective labeling of receptor proteins with FIAsh. White scale bars represent 10 μ m.

GPCRs, like the adenosine A_{2A} receptor,¹³ the α_{2A} -adrenergic receptor,^{14,16} the β_1 adrenergic receptor,²⁰ or the M_2 -ACh receptor,¹⁷ receptor binding and signaling to G-proteins remained intact in our new constructs (data not shown).

2.2. The mACh receptor sensors report conformational changes in response to orthosteric ligands

For FRET experiments we used single HEK-293 cells, which showed clear membrane localization and FIAsh labeling of the receptor sensor as depicted in Figure 1B. To stimulate cells we used acetylcholine, carbachol, oxotremorine M, and muscarine, thus four well-characterized agonists for mACh receptors. The chemical structures of these compounds are shown in Figure 2. For each receptor construct stimulation of fluorescent cells with the receptor agonists resulted in a fast, reversible increase in FIAsh and a concomitant decrease in CFP fluorescence, indicative of an increase in FRET (Figs. 3A, 4A and 5A). The changes in CFP and FIAsh fluorescence were clearly agonist-dependent and had maximal amplitudes of ~8–10%, for each construct, which can be easily measured without visible desensitization of the FRET signals even after multiple stimulations. Next, we used various concentrations of four mACh receptor agonists to establish concentration–response curves for each agonist at each receptor construct. In Figure 3A representative traces of an individual experiment using increasing concentrations of acetylcholine at the M_1 -ACh receptor construct are shown. From these data concentration–response curves were calculated by using maximal saturating concentrations of acetylcholine as the reference. The detected changes in FRET ratio for each concentration were normalized to the maximal change observed for acetylcholine and plotted against the agonist concentration. As shown in Figure 3B, we observed a concentration-dependent increase in FRET-changes for the different agonists used. From these curves, EC_{50} -values between 1 and 30 μ M, respectively (Fig. 3B) were obtained. These data are in good agreement with published data for low affinity binding,^{21–25} at the muscarinic receptor subtypes. However, these values are high compared to potencies determined from functional experiments, but it must be kept in mind that in the FRET experiments there is no receptor reserve and they are measured under non-equilibrium conditions.

Similar experiments were performed for the M_3 - and M_5 -ACh receptor constructs and representative data of individual experiments are shown in Figures 4A and 5A. Likewise, concentration-dependent effects were determined as described for the M_1 -ACh receptor sensor and FRET-changes were normalized to maximal effects of acetylcholine and plotted the against agonist concentra-

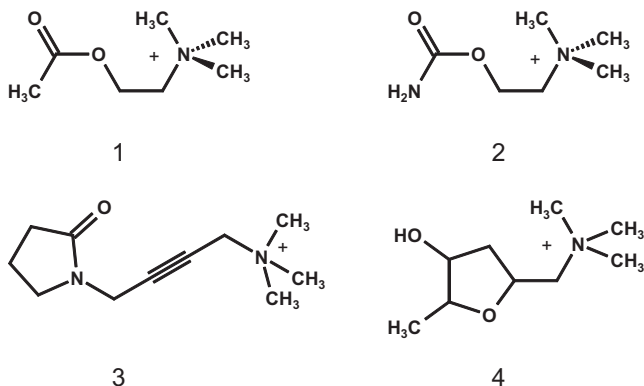


Figure 2. Chemical structures of the agonists used in this study. Acetylcholine (1), carbachol (2), oxotremorine M (3), muscarine (4). These numbers are used throughout the manuscript for the substances as indicated.

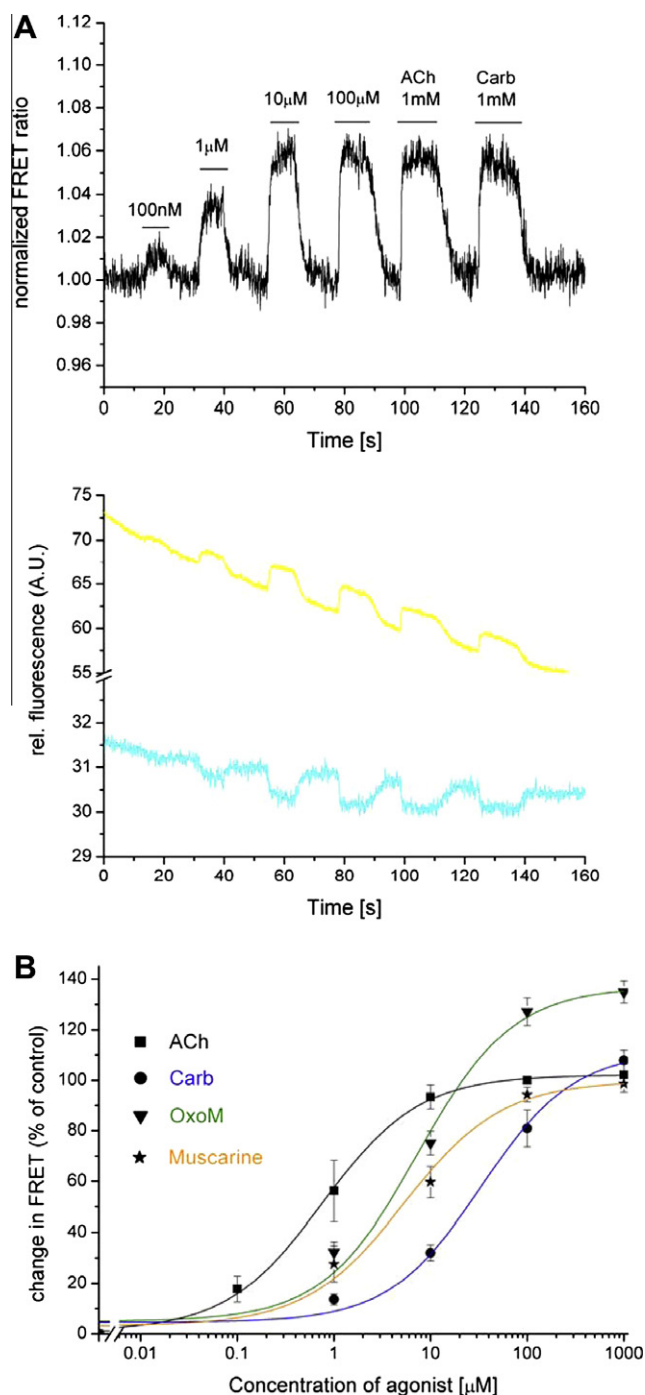


Figure 3. Effects of agonists on the FRET-response of the M_1 -ACh receptor sensor. Fluorescence emission was measured at 480 nm (CFP, cyan color) and at 535 nm (FIAsh, yellow color) from cells expressing the M_1 -ACh receptor sensor and superfused for the indicated period of time with agonist. (A) Individual recording from a single cell shows that acetylcholine induced a rapid decrease in CFP and a corresponding increase in FIAsh fluorescence intensity (lower panel), resulting in an increased ratio F_{535}/F_{480} , representing FRET (upper panel). Upon wash-out of acetylcholine all traces reverted to their original values. (B) Concentration–response curves for the FRET-changes evoked by acetylcholine, carbachol, oxotremorine M, and muscarine revealed EC_{50} -values of 0.77 ± 0.07 μ M, 33.5 ± 9.6 μ M, 7.4 ± 2.4 μ M, and 5.3 ± 1.9 μ M, respectively (means \pm SE, $n = 10$ –14).

tions. The resulting data are shown in Figures 4B and 5B, respectively. The observed EC_{50} -values for the M_3 -ACh receptor sensor or the M_5 -ACh receptor sensor were between 0.5 and 3 μ M, and 1 and 5 μ M respectively (Fig 4B and 5B). Again these

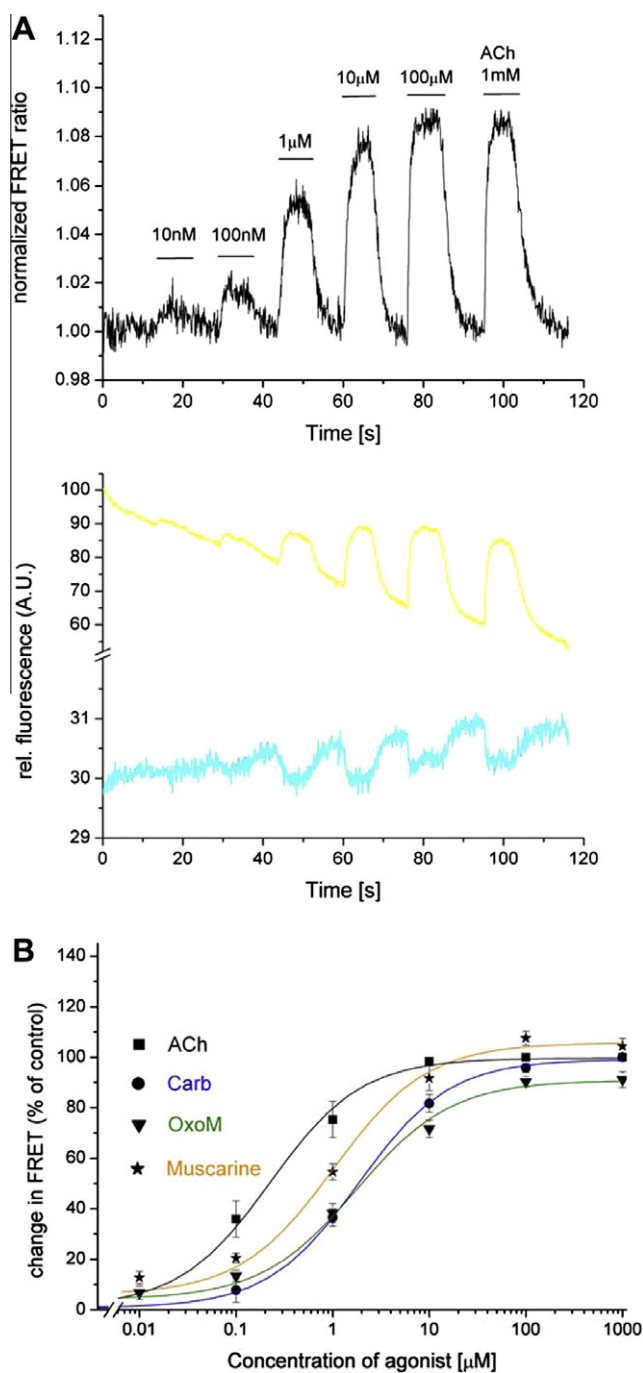


Figure 4. Effects of agonists on the FRET-response of the M_3 -ACh receptor sensor. Fluorescence emission was measured at 480 nm (CFP, cyan color) and at 535 nm (FIAsh, yellow color) from cells expressing the M_3 -ACh receptor sensor and superfused for the indicated period of time with agonist. (A) Individual recording from a single cell shows that acetylcholine induced a rapid decrease in CFP and a corresponding increase in FIAsh fluorescence intensity (lower panel), resulting in an increased ratio F_{535}/F_{480} , representing FRET (upper panel). Upon wash-out of acetylcholine all traces reverted to their original values. (B) Concentration–response curves for the FRET-changes evoked by acetylcholine, carbachol, oxotremorine M, and muscarine revealed EC_{50} -values of $0.22 \pm 0.04 \mu\text{M}$, $1.9 \pm 0.1 \mu\text{M}$, $1.8 \pm 0.3 \mu\text{M}$, and $1.0 \pm 0.2 \mu\text{M}$, respectively (means \pm SE, $n = 12$ –15).

data are in good agreement with published data for low affinity binding.^{21–25} When the data for the individual muscarinic receptors were compared, we observed the following relative potencies;

M_1 -ACh receptor: ACh > Muscarine = OxoM > Carb

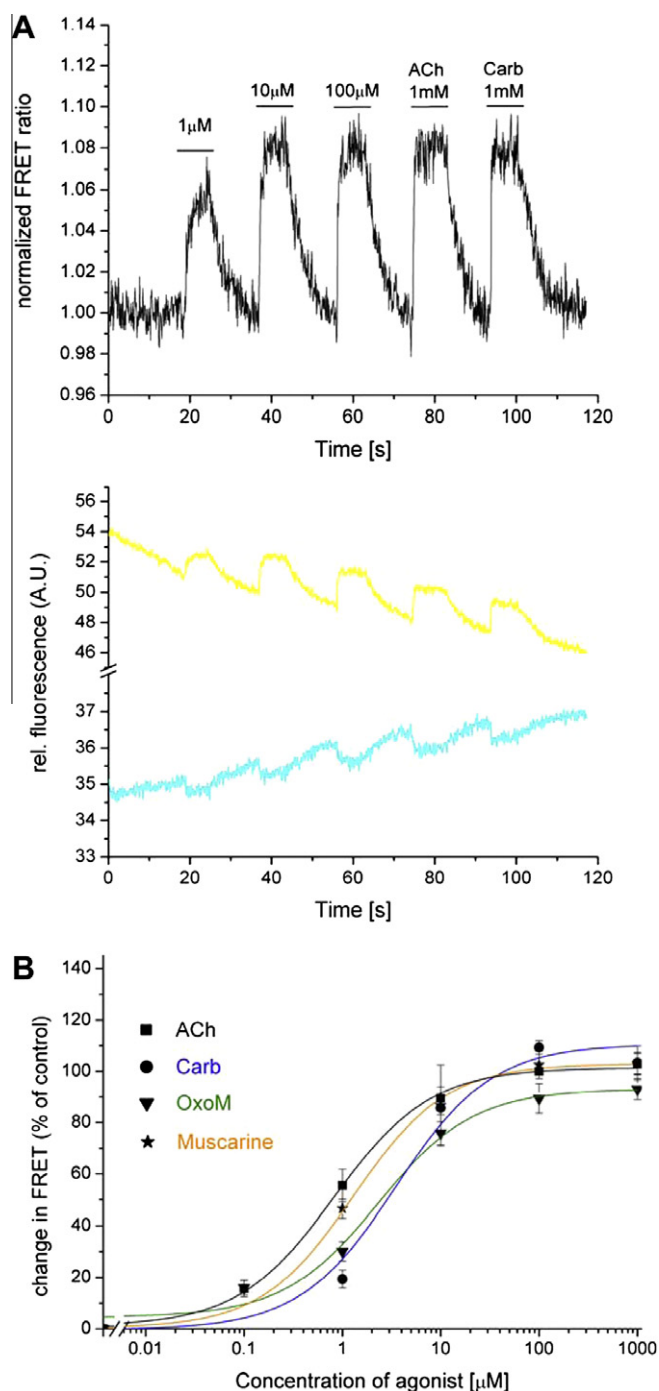


Figure 5. Effects of agonists on the FRET-response of the M_5 -ACh receptor sensor. Fluorescence emission was measured at 480 nm (CFP, cyan color) and at 535 nm (FIAsh, yellow color) from cells expressing the M_5 -ACh receptor sensor and superfused for the indicated period of time with agonist. (A) Individual recording from a single cell shows that acetylcholine induced a rapid decrease in CFP and a corresponding increase in FIAsh fluorescence intensity (lower panel), resulting in an increased ratio F_{535}/F_{480} , representing FRET (upper panel). Upon wash-out of acetylcholine all traces reverted to their original values. (B) Concentration–response curves for the FRET-changes evoked by acetylcholine, carbachol, oxotremorine M, and muscarine revealed EC_{50} -values of $0.79 \pm 0.12 \mu\text{M}$, $2.8 \pm 0.9 \mu\text{M}$, $2.3 \pm 1.0 \mu\text{M}$, and $1.3 \pm 0.2 \mu\text{M}$ respectively (means \pm SE, $n = 11$ –13).

M_3 -ACh receptor: ACh > Muscarine > OxoM = Carb
 M_5 -ACh receptor: ACh = Muscarine > OxoM = Carb

Thus, each receptor subtype revealed its own slightly different agonist profile.

2.3. Kinetics of agonist induced conformational changes

Since our FRET-based approach represents a unique tool to monitor changes in receptor conformation in real time, we analyzed the kinetics of the different orthosteric ligands used in this study. As in the preceding experiments, single cells were superfused with an agonist, acetylcholine, carbachol, oxotremorine M, or muscarine, at saturating concentrations of 100 μ M or in some cases 1 mM. Saturating concentrations are necessary for these experiments since we have previously shown that the speed of the conformational change is concentration-dependent^{12–14} and thus maximal only when the receptor is fully activated. The data were recorded at a frequency of 20–50 Hz, thus allowing a good kinetic resolution of the signal change. In Figure 6A–C sample data are shown for the M₁-ACh receptor, M₃-ACh receptor, and the M₅-ACh receptor stimulated with ACh or OxoM. When comparing the data for the three individual receptor subtypes it can be seen that all receptors are activated with τ -values of 90 ms, which reflect half-maximal activation times of 60 ms for the receptor constructs. Interestingly, when comparing the kinetic data for each receptor (see Fig. 6 and Table 1), significant inter-individual differences can be seen between the different receptor subtypes for OxoM, while the other agonists behaved very similar at each receptor tested. In Table 1 kinetic data for each ligand are summarized as half-maximal activation times and corresponding rate constants at the three receptors tested.

3. Discussion

In this paper, we describe the generation of three FRET-sensor constructs for the G_q-coupled muscarinic acetylcholine receptor subtypes M₁-, M₃-, and M₅-AChR. We chose FAsH as the acceptor fluorophore since earlier studies with other receptors, had shown that FAsH, compared to YFP, provided higher signal amplitudes and preserved the receptor functionality in terms of activation of downstream signaling.^{13,16,17} The constructs were designed in accordance to the recently published M₂-ACh receptor sensor¹⁷ (Fig. 1A). All constructs were well expressed in HEK-293 cells and were located at the plasma membrane (Fig. 1B) and specific labeled with FAsH. Unlike the M₂-ACh receptor sensor, which showed a decrease in the FRET signal upon agonist exposure, all three G_q-coupled sensors exhibited a strong and rapid increase in the FRET signal (Fig. 3–5) when stimulated with agonists. This is a striking difference given the high sequence homology of the muscarinic acetylcholine receptors.²⁶ This difference might rather be due to different orientation factors between the two fluorophores rather than different movements of the helices upon receptor activation. The general activation mechanism within the GPCR family appears rather conserved^{27–30} and thus makes it unlikely that a different mechanism of activation has evolved within the receptor family. Furthermore, two recently published M₁-ACh receptor sensors based on CFP/YFP fluorophore combinations were characterized by an increase³¹ or decrease in FRET upon agonist application.³² These reports thus strengthen the notion of a possible influence of orientation factors in the observed change of the FRET signals. Similar to previous reports,¹³ the combination of FAsH and CFP at the M₁-ACh receptor provides much higher signal amplitudes compared to CFP/YFP (approximately 8% agonist induced FRET-change versus 1.5%³¹).

Receptor activation for the muscarinic M₁-, M₃-, and M₅-ACh receptor sensors occurred rapidly at saturating agonist concentration and in the millisecond time range. The three sensors described here exhibit half-maximal activation times of 60–70 ms and hence rate constants of 15–17 s⁻¹ (Fig. 6 and Table 1). Thus, for stimulation with the endogenous receptor agonist the data are in excellent

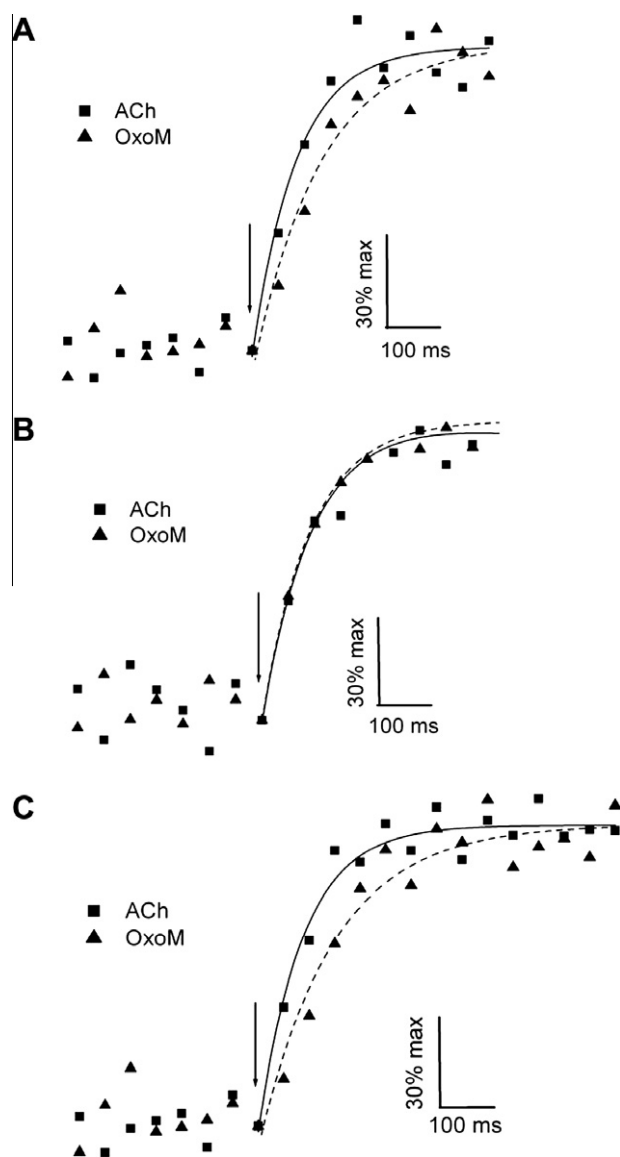


Figure 6. Kinetics of agonist mediated changes in the FRET ratio. HEK-293 cells transfected with the corresponding mAChR receptor sensor were superfused with saturating agonist concentrations (100 μ M or 1 mM). Recordings were done on single cells with 20–50 Hz and the kinetics of the change in FRET were analyzed by exponential fitting. Individual signal traces for maximal stimulation with acetylcholine or oxotremorine M were normalized to 100 percent signal strength and an overlay of these signal traces is shown. Figure A shows a representative data sample and exponential fit for the M₁-ACh receptor construct superfused with acetylcholine (black squares and solid line) or oxotremorine M (black triangle and dashed line). Figure B shows a representative data sample and exponential fit for the M₃-ACh receptor construct superfused with acetylcholine (black squares and solid line) or oxotremorine M (black triangle and dashed line). Figure C shows a representative data sample and exponential fit for the M₅-ACh receptor construct superfused with acetylcholine (black squares and solid line) or oxotremorine M (black triangle and dashed line).

agreement with previously published values for activation of other GPCRs.^{13,14,16,17,31} A concentration-dependent change in the amplitude of the FRET signal was observed for all agonist tested and the data were normalized to the maximal signal observed with acetylcholine for each receptor. The obtained data are given in Figures 3B, 4B and 5B for each individual receptor sensor. From these curves EC₅₀-values were calculated and the obtained data are in good agreement with previously published binding affinities of the corresponding muscarinic receptor subtype in the presence of

Table 1
Kinetics of agonist mediated changes in the FRET ratio

Ligand	M ₁ -ACh receptor		M ₃ -ACh receptor		M ₅ -ACh receptor	
	Activation time $t_{1/2}$ [ms]	Rate constant [s^{-1}]	Activation time $t_{1/2}$ [ms]	Rate constant [s^{-1}]	Activation time $t_{1/2}$ [ms]	Rate constant [s^{-1}]
ACh	59.4 ± 4.1	16.8	62.4 ± 5.8	16.0	65.0 ± 7.6	15.4
Carbachol	58.7 ± 4.3	17.0	62.7 ± 5.6	15.9	68.0 ± 6.9	14.7
Oxo M	74.4 ± 6.4*	13.4	64.4 ± 7.1	15.5	104.0 ± 9.9**	9.6
Muscarine	70.1 ± 8.2	14.3	66.8 ± 5.8	15.0	72.1 ± 10.1	13.9

HEK-293 cells transfected with the corresponding mAChR receptor sensor were superfused with saturating agonist concentrations (100 μ M or 1 mM). Recordings were done on single cells with 20–50 Hz and the kinetics of the change in FRET were analyzed by exponential fitting. Half-maximal activation times for each ligand were analyzed at maximal receptor stimulation and full receptor occupancy. The given rate constants were calculated using the corresponding half-maximal activation times as $1/\text{activation time}$. M₁-ACh receptor construct: $n = 12$ –15 for each ligand; M₃-ACh receptor construct: $n = 16$ –24 for each ligand; M₅-ACh receptor construct: $n = 12$ –17 for each ligand. The results represent the mean ± s.e.m. of the indicated number of independent experiments.

* $p < 0.05$.

** $p < 0.01$ independent t -test).

GTP.^{21,25} These values may appear high when compared to potencies determined from functional experiments. However, as mentioned earlier, one needs to keep in mind that there is no receptor reserve in the FRET experiments and that they are measured under non-equilibrium conditions. From previous studies we know that partial agonists induce smaller signal amplitudes than full agonists.^{16,17} Consistent with that observation, all four compounds tested here induced similar changes in FRET signal amplitudes, and have previously been described as full agonists for the stimulation of inositol phosphate production³³ or MAP-kinase pathway activation³⁴ for all three receptor subtypes. However, as an exception we observed that Oxo M induced a significantly larger change in FRET at the M₁-ACh receptor sensor compared to the endogenous agonist acetylcholine ($p < 0.01$, Student t -test, Fig. 3b). However, the receptor activation with Oxo M, even at maximally saturating conditions of 1 mM, occurred significantly slower compared to acetylcholine ($p < 0.05$, Student t -test, Fig. 6). Unlike the M₁-ACh receptor, at the M₃- and M₅-ACh receptor sensors Oxo M induced the same change in FRET amplitude as compared to acetylcholine (Figs. 4B and 5B). Most interestingly, the kinetics of signal change were different at both receptors with OxoM being as fast as acetylcholine at the M₃-ACh receptor but being the slowest compound tested at the M₅-ACh receptor ($p < 0.01$, Student t -test, Fig. 6 and Table 1). A larger but slower change in FRET has not been observed previously, but slower conformational changes have so far been consistent with differential conformational changes upon ligand stimulation.^{14,16,35,36}

4. Conclusion

In conclusion, the receptor sensors described in this manuscript reveal novel insights into muscarinic receptor activation and the observed agonist activation patterns are consistent with previously published pharmacological characteristics of the corresponding wild-type muscarinic receptor subtypes. Thus, these novel receptor sensors may provide useful tools to study receptor activation in real time and with high kinetic resolutions, which could previously not be accessed by other techniques and may help to further develop selective compounds for muscarinic receptor modulation.

5. Materials and methods

5.1. Materials

Acetylcholine, muscarine, and poly-D-lysine were purchased from Sigma (Steinheim, Germany). Oxotremorine M was obtained from Tocris (Bristol, UK). Carbachol was purchased from Alfa Aesar (Karlsruhe, Germany). Cell culture reagents were supplied by PAN-Biotech GmbH (Aidenbach, Germany). Effectene was purchased

from Quiagen (Hilden, Germany). cDNA for the human muscarinic M₁-, M₃-, and M₅-acetylcholine receptors was obtained from the cDNA resource center, University of Missouri-Rolla (Rolla, MO, USA). All PCR primers were synthesized by MWG-Biotech GmbH (Ebersberg, Germany). All other chemicals were purchased from commercial suppliers at the highest purity grade available.

5.2. Construction of the muscarinic FRET-sensor constructs

Muscarinic ACh receptor constructs were fused to the enhanced variants of cyan fluorescent protein (eCFP) (BD Bioscience Clontech, Heidelberg, Germany) by standard PCR extension overlap technique.³⁷ All constructs were verified by sequencing and sequencing was done by Eurofins Medigenomix GmbH (Martinsried, Germany). In each case, the C-terminal stop-codon of the receptor and the initial codon for methionine of the fluorescent protein were deleted. The amino acid sequence SR, coding for an Xba I restriction site, was inserted as a linker sequence between the receptor and the fluorescent protein. For each individual muscarinic receptor construct an additional modification was made to the third intracellular loop (IL3) by deleting a large portion of the loop and replacing it with a short amino acid motif CCPGCC which specifically binds the fluoresceine arsenical hairpin binder (FIAsH). The IL3 of the M₁-ACh receptor was deleted between amino acids 228 and 350, and the novel sequence of this part reads: LAALQCG²²⁸CCPGCCSGK³⁵⁰PRGKE. In case of the M₃-ACh receptor, the IL3 was deleted between amino acids 271 and 465, and the novel sequence of this part reads: LAGLQA²⁷¹CCPGCCF⁴⁶⁵ALKTRS. Finally, the IL3 of the M₅-ACh receptor was deleted between amino acids 233 and 422, and the novel sequence of this part reads: KDLADLQ²³³GCCPGCCSGN⁴²²PNPSH. All resulting constructs were cloned into pcDNA3 (Invitrogen) and confirmed by sequencing.

5.3. Cell culture

HEK-293 cells were maintained in DMEM with 4.5 g/l glucose, 10% FCS, 100 U/ml penicillin G and 100 μ g/ml streptomycin sulfate at 37 °C, 7% CO₂. All cells were routinely passaged every two to three days. Culture medium for cells stably expressing the individual mACh receptor constructs was additionally supplemented with 200 μ g/ml G-418.

5.4. Transfection of HEK-293 cells for microscopic analysis

Individual 24 mm glass cover slips were placed in six-well plates and coated for 30–60 min using 300 μ l of poly-D-lysine (1 mg/ml). Poly-D-lysine was aspirated and the glass cover slips were washed once with sterile PBS without Ca²⁺. HEK-293 cells were seeded onto these cover slips to result in approximately

50% confluence. After attachment of the cells (3–6 h), the cells were transfected using Effectene (Quiagen) according to the manufacturer's instructions. 250 ng DNA per well were used for transfection of each receptor construct and cell culture medium was exchanged 12–16 h later. Cells were analyzed 48 h after transfection.

5.5. Confocal microscopy

Confocal microscopy experiments were performed on a Leica TCS SP2 system. Cover slips with transfected HEK-293 cells were mounted using an Attofluor holder (Molecular Probes, Leiden, The Netherlands). Images were taken with a 63× objective as described previously.³⁸ In brief, CFP was excited with a 430 nm diode laser using a DCLP455 dichroic mirror. FIAsh was excited using the 514 nm argon laser line using the manufacturers setting for YFP. Settings for recording images were kept constant: 512 × 512 pixel format, line average 4, 400 Hz, resulting in an image acquisition time of 7 s.

5.6. FIAsh labeling

The labeling was performed as described previously.^{13,16} In brief, transfected cells were washed twice on the cover slips with phenol red-free Hank's balanced salt solution containing 1 g/l glucose (HBSS, 137 mM NaCl, 5.4 mM KCl, 0.3 mM Na₂HPO₄, 0.4 mM KH₂PO₄, 4.2 mM NaHCO₃, 1.3 mM CaCl₂, 0.5 mM MgCl₂, 0.6 mM MgSO₄, 5.6 mM glucose, pH 7.4) and then incubated at 37 °C for 1 h with HBSS containing 500 nM FIAsh and 12.5 μM 1,2-ethane dithiol (EDT). Subsequently, to reduce non-specific labeling, the cells were washed twice with HBSS, incubated for 10 min with HBSS/250 μM EDT and again washed twice before being used for fluorescence measurements.

5.7. Fluorescence resonance energy transfer (FRET) experiments

Fluorescence imaging of FIAsh labeled mACh receptor sensors was performed as previously described^{12,13} on a Zeiss Axiovert 135 inverted microscope equipped with a Zeiss PlanNeofluar 100×/1.3 oil objective at room temperature. Samples were excited at 436 nm (dichroic 450 nm) with light from a polychrome IV (Till Photonics). The light source settings were controlled by Till pmc Communications software version 1.0.5. The emission ratio (FIAsh over eCFP) was measured with emission filters 480/40 nm (eCFP) and 535/30 nm (FIAsh), beam splitter DCLP 505 nm. Signals detected by photodiodes were digitized using an AD converter (Digidata1322A, Axon Instruments) and stored on PC using Clampex 8.1 software (Axon Instruments).

The emission ratio was corrected offline for bleed-through of eCFP into the FIAsh channel to give a corrected emission ratio (bleed-through of FIAsh into the eCFP channel is negligible). FIAsh emission after excitation with light at 490 nm was determined in order to subtract direct excitation of FIAsh. To study ligand-induced changes in FRET, cells were continuously superfused with imaging buffer (140 mM NaCl, 5.4 mM KCl, 2 mM CaCl₂, 1 mM MgCl₂, 10 mM HEPES, pH 7.3) supplemented with various ligands and concentrations thereof as indicated, applied with the help of a computer-assisted solenoid valve-controlled rapid superfusion device ALA-VM8 (ALA Scientific Instruments; solution exchange in 5–10 ms).

5.8. Data processing

Fluorescence intensities were acquired using Clampex (Axon Instruments). Values are given as mean ± s.e.m. of n independent experiments. Statistical analysis and curve fitting were performed using Origin (OriginLab) or Clampfit (Axon Instruments).

Acknowledgments

We thank Christian Dees for expert technical assistance and Nadine Frölich, Susanne Reiner, Alexander Zürn and Viacheslav O. Nikolaev for helpful discussions. This work was funded by the Deutsche Forschungsgemeinschaft (SFB487; TPA1; to M.J.L. and C.H.).

References and notes

- Fredriksson, R.; Schioth, H. B. *Mol. Pharmacol.* **2005**, *67*, 1414.
- Wess, J.; Eglén, R. M.; Gautam, D. *Nat. Rev. Drug Disc.* **2007**, *6*, 721.
- van Koppen, C. J.; Kaiser, B. *Pharmacol. Ther.* **2003**, *98*, 197.
- Eglén, R. M. *Prog. Med. Chem.* **2005**, *43*, 105.
- Christopoulos, A. *Nat. Rev. Drug Disc.* **2002**, *1*, 198.
- May, L. T.; Leach, K.; Sexton, P. M.; Christopoulos, A. *Annu. Rev. Pharmacol. Toxicol.* **2007**, *47*, 1.
- Gregory, K. J.; Sexton, P. M.; Christopoulos, A. *Curr. Neuropharmacol.* **2007**, *5*, 157.
- Birdsall, N. J.; Lazareno, S. *Mini-Rev. Med. Chem.* **2005**, *5*, 523.
- De Amici, M.; Dallanocce, C.; Holzgrabe, U.; Trankle, C.; Mohr, K. *Med. Res. Rev.* **2010**, *30*, 463.
- Mohr, K.; Trankle, C.; Kostenis, E.; Barocelli, E.; De Amici, M.; Holzgrabe, U. *Br. J. Pharmacol.* **2010**, *159*, 997.
- Ehlert, F. J. *J. Pharmacol. Exp. Ther.* **2005**, *315*, 740.
- Vilardaga, J. P.; Bunemann, M.; Krasel, C.; Castro, M.; Lohse, M. J. *Nat. Biotechnol.* **2003**, *21*, 807.
- Hoffmann, C.; Gaietta, G.; Bunemann, M.; Adams, S. R.; Oberdorff-Maass, S.; Behr, B.; Vilardaga, J. P.; Tsien, R. Y.; Ellisman, M. H.; Lohse, M. J. *Nat. Methods* **2005**, *2*, 171.
- Nikolaev, V. O.; Hoffmann, C.; Bunemann, M.; Lohse, M. J.; Vilardaga, J. P. *J. Biol. Chem.* **2006**, *281*, 24506.
- Adams, S. R.; Campbell, R. E.; Gross, L. A.; Martin, B. R.; Walkup, G. K.; Yao, Y.; Llopis, J.; Tsien, R. Y. *J. Am. Chem. Soc.* **2002**, *124*, 6063.
- Zurn, A.; Zabel, U.; Vilardaga, J. P.; Schindelin, H.; Lohse, M. J.; Hoffmann, C. *Mol. Pharmacol.* **2009**, *75*, 534.
- Maier-Puschel, M.; Frölich, N.; Dees, C.; Hommers, L. G.; Hoffmann, C.; Nikolaev, V. O.; Lohse, M. J. *J. Biol. Chem.* **2010**, *285*, 8793.
- Wess, J. *Pharmacol. Ther.* **1998**, *80*, 231.
- Zeng, F. Y.; Hopp, A.; Soldner, A.; Wess, J. *J. Biol. Chem.* **1999**, *274*, 16629.
- Rochais, F.; Vilardaga, J. P.; Nikolaev, V. O.; Bunemann, M.; Lohse, M. J.; Engelhardt, S. *J. Clin. Invest.* **2007**, *117*, 229.
- Jakubik, J.; Bacakova, L.; El-Fakahany, E. E.; Tucek, S. *Mol. Pharmacol.* **1997**, *52*, 172.
- Caulfield, M. P.; Birdsall, N. J. *Pharmacol. Rev.* **1998**, *50*, 279.
- Wood, M. D.; Murkitt, K. L.; Ho, M.; Watson, J. M.; Brown, F.; Hunter, A. J.; Middlemiss, D. N. *Br. J. Pharmacol.* **1999**, *126*, 1620.
- Eglén, R. M.; Nahorski, S. R. *Br. J. Pharmacol.* **2000**, *130*, 13.
- Thomas, R. L.; Langmead, C. J.; Wood, M. D.; Challiss, R. A. J. *Pharmacol. Exp. Ther.* **2009**, *331*, 1086.
- Wess, J. *Crit. Rev. Neurobiol.* **1996**, *10*, 69.
- Hoffmann, C.; Zurn, A.; Bunemann, M.; Lohse, M. J. *Br. J. Pharmacol.* **2008**, *153*, S358.
- Nygaard, R.; Frimurer, T. M.; Holst, B.; Rosenkilde, M. M.; Schwartz, T. W. *Trends Pharmacol. Sci.* **2009**, *30*, 249.
- Tate, C. G.; Schertler, G. F. *Curr. Opin. Struct. Biol.* **2009**, *19*, 386.
- Rosenbaum, D. M.; Rasmussen, S. G.; Kobilka, B. K. *Nature* **2009**, *459*, 356.
- Jensen, J. B.; Lyssand, J. S.; Hague, C.; Hille, B. *J. Gen. Physiol.* **2009**, *133*, 347.
- Matsushita, S.; Nakata, H.; Kubo, Y.; Tateyama, M. *J. Biol. Chem.* **2010**, *285*, 10291.
- Wang, S. Z.; el-Fakahany, E. E. *J. Pharmacol. Exp. Ther.* **1993**, *266*, 237.
- Wotta, D. R.; Wattenberg, E. V.; Langason, R. B.; el-Fakahany, E. E. *Pharmacology* **1998**, *56*, 175.
- Lohse, M. J.; Nikolaev, V. O.; Hein, P.; Hoffmann, C.; Vilardaga, J. P.; Bunemann, M. *Trends Pharmacol. Sci.* **2008**, *29*, 159.
- Vilardaga, J. P.; Bunemann, M.; Feinstein, T. N.; Lambert, N.; Nikolaev, V. O.; Engelhardt, S.; Lohse, M. J.; Hoffmann, C. *Mol. Endocrinol.* **2009**, *23*, 590.
- Ho, S. N.; Hunt, H. D.; Horton, R. M.; Pullen, J. K.; Pease, L. R. *Gene* **1989**, *77*, 51.
- Hoffmann, C.; Ziegler, N.; Reiner, S.; Krasel, C.; Lohse, M. J. *J. Biol. Chem.* **2008**, *283*, 30933.